BNL-211135-2019-TECH

NSLSII-ASD-TN-157

NSLS-II Emittance and Lifetime with Damping Wigglers

T. Shaftan,

January 2015

Photon Sciences

Brookhaven National Laboratory

U.S. Department of Energy

USDOE Office of Science (SC), Basic Energy Sciences (BES) (SC-22)

DISCLAIMER

NSLS II TECHNICAL NOTE BROOKHAVEN NATIONAL LABORATORY	NUMBER: **NSLSII-ASD-TN-157**
AUTHOR **T. Shaftan, G. Wang, P. Ilinsky and W. Guo**	DATE **1/04/2015**
TITLE **NSLS-II emittance and lifetime with Damping Wigglers**	

January 4, 2015

Abstract

This paper is focused on the measurements of the major machine parameters under influence of the Damping Wigglers and their comparison with analytic estimates. We present analysis of the impact of the Damping Wigglers on the beam emittance and lifetime in the NSLS-II storage ring. We conclude that these parameters for the NSLS-II follow well-known dependencies as described, for example, by Weidemann [1] and Touschek [2, 3, 4, 5]. Appendices A and B show details of the experiment and the estimates.

NSLS-II lattice

The analysis carried out in this paper relies on the actual machine lattice [6] set-up. The linear machine model was validated through beam measurements of beta-functions, phase advances, tunes and chromaticity. To the date of this experiment the linear lattice functions were symmetrized and known to the accuracy of 2-3% with respect to the model values.

The machine beam sizes and Twiss functions with their fits are depicted on Fig. 1. The beam sizes are calculated using the designed beam emittance of 2.05 nm·rad and 0.051% energy spread rad at 3 GeV with no DWs. The marker at 19.3 m indicates position of the X-ray diagnostics. Markers on the vertical scale correspond to the average beam sizes along the machine used in the Touschek lifetime calculations.

Twiss functions and Courant-Snider invariant are plotted in the right window of Fig. 1. The vertical markers indicate values of the beta-functions at the location of the X-ray diagnostics. These values were used for the beam emittance measurements.

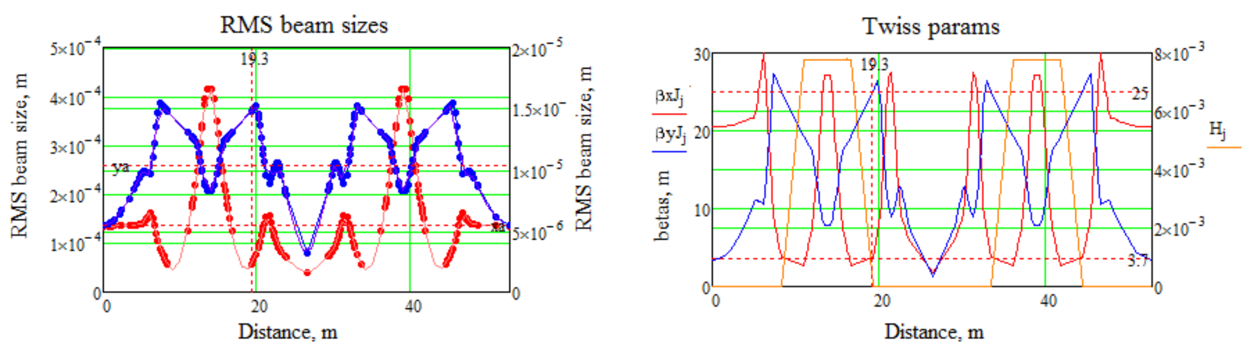

Fig. 1: NSLS-II beam sizes along a single cell (left). Beta-functions and the Courant invariant (right).

The figures above correspond to the “bare” lattice, i.e. without Damping Wiggler (DW) gaps closed. The following plots (Fig. 2) illustrate distortion of the beta-functions due to different number of DWs.

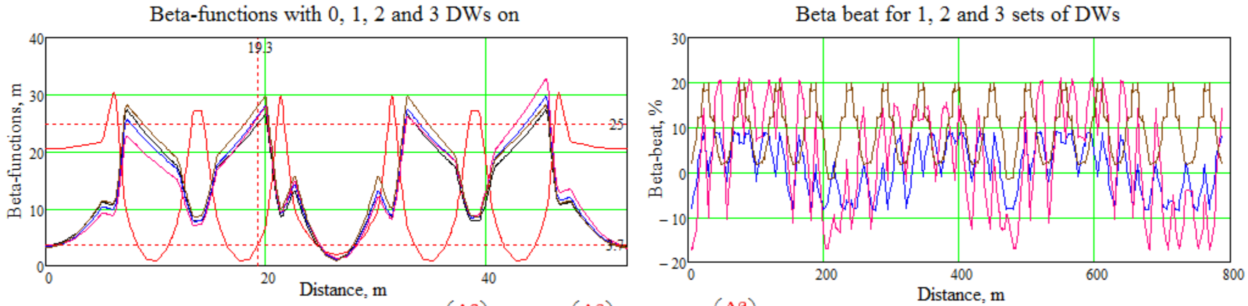

$\left(\frac{\Delta\beta}{\beta}\right)_1 := 6.06\% \quad \left(\frac{\Delta\beta}{\beta}\right)_{12} := 12.1\% \quad \left(\frac{\Delta\beta}{\beta}\right)_{123} := 5.66\%$

Fig 2: Distortion of the vertical beta-function relative to the number of engaged DWs (left). Resulted beta-beat for the uncorrected lattice (right).

RMS distortion of the lattice functions increases by 6% as the gaps of first two 7 m long DWs are closed. After closing the third 7-m long DW the distortion reduces to 5% as the lattice symmetry is somewhat restored. The distortion takes place in the vertical plane, so that the impact on the horizontal beam size is insignificant. At the location of the X-ray diagnostics (Fig. 2) the vertical beta-function changes within 5-10% range and, thus, the horizontal beam size should not change as a function of the closed DWs.

The major effect from closing all DW gaps is depicted below. We calculate the impact of L_W (total DW length in meters) of DW on the emittance and energy spread [1].

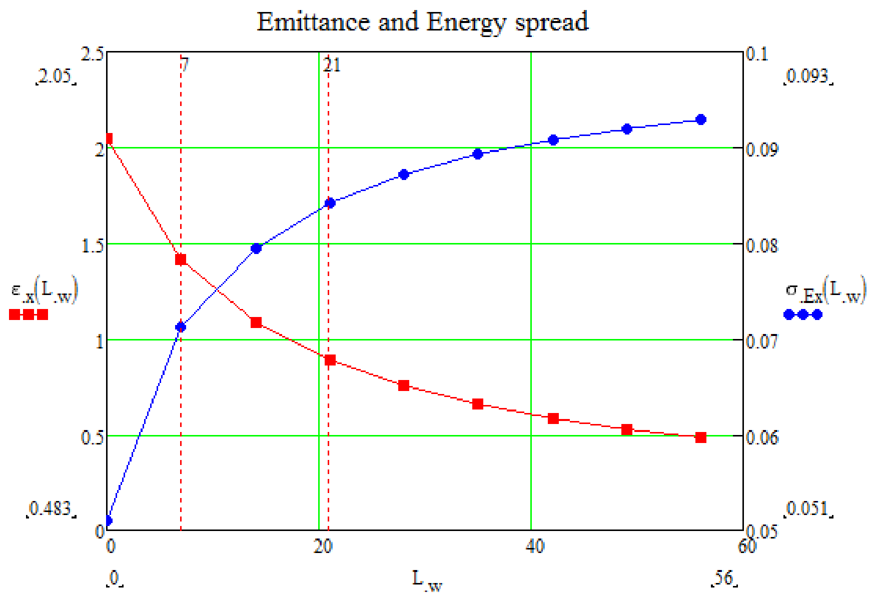

Fig 3: Theoretical value of emittance (red curve) and energy spread (blue curve) as a function of the total DW length.

The dependence begins from L_W=0, where the emittance and energy spread correspond to the bare lattice values of 2.05 nm·rad and 0.051% energy spread. With the compliment of three seven meter long DWs installed in cells 8, 18 and 28 the emittance reaches the design value of 0.885 nm·rad, while energy spread grows to 0.084%.

Measurements of the beam sizes and the horizontal emittance

We used X-ray diagnostics for measurements of the beam size at the entrance of the first bending magnet (BM-A) in the achromat, which is located at the machine azimuth with zero dispersion.

X-ray diagnostics [7] is based on imaging of the bending magnet synchrotron radiation in the range of 5 mA to 500 mA of the stored electron beam current. Imaging requires spatial resolution of the diagnostics to be better than three microns in order to observe changes of the vertical beam size. Flux from bending magnet is attenuated by 1-mm-thick aluminum window and 10-m-long air path. X-ray diagnostics is setup in air. For optimal resolution and flux performance operation energy is set at 20 keV X-ray radiation from the source is imaged onto the fluorescent crystal, which converts x-rays into visible light photons, visible light imaged then onto the CCD chip by micro-objective.

We took two sets of measurements at the beam current of 1.5 mA closing DWs in the following sequence: #1 (all closed, 18 and 28 closed, 28 closed, all open) and #2 (all open, 18 closed, 8 and 18 closed, all closed). Then the horizontal emittance value was retrieved using the beta-function value described in the section above. Figure 4 demonstrates the outcome of this experiment indicating good agreement with expectations (red curve corresponds to analytic estimate from Fig. 3 within 0…21 m range of L_w).

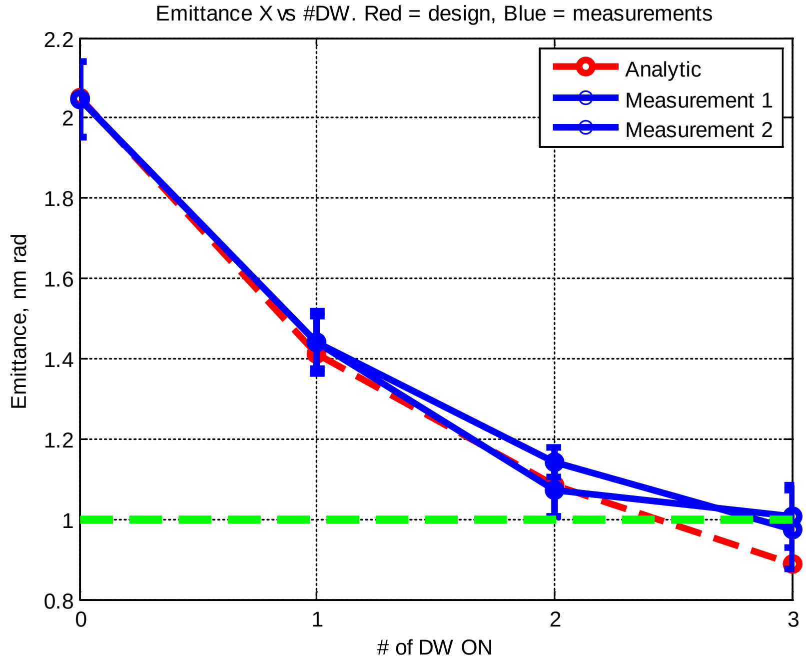

Fig. 4: Experimental results: blue curves correspond to the two sets of measurements vs theoretical estimate. Green line corresponds to the project goal of 1 nm.

Attempt has been made to retrieve the energy spread from the beam size measurements at the visual synchrotron diagnostics. However the latter exhibited high degree of jitter both in the beam size and in the beam position so that consistent measurements were not possible.

Vertical beam size was recorded from the X-ray diagnostics as well (Fig. 5). We found that the beam size changed very substantially between closing different combinations of the DWs. For instance, closing gap of DW cell 18 alone has doubled it, while including DWs in cells 8 and 18 reduced the vertical size half way with respect to the “bare” lattice scenario.

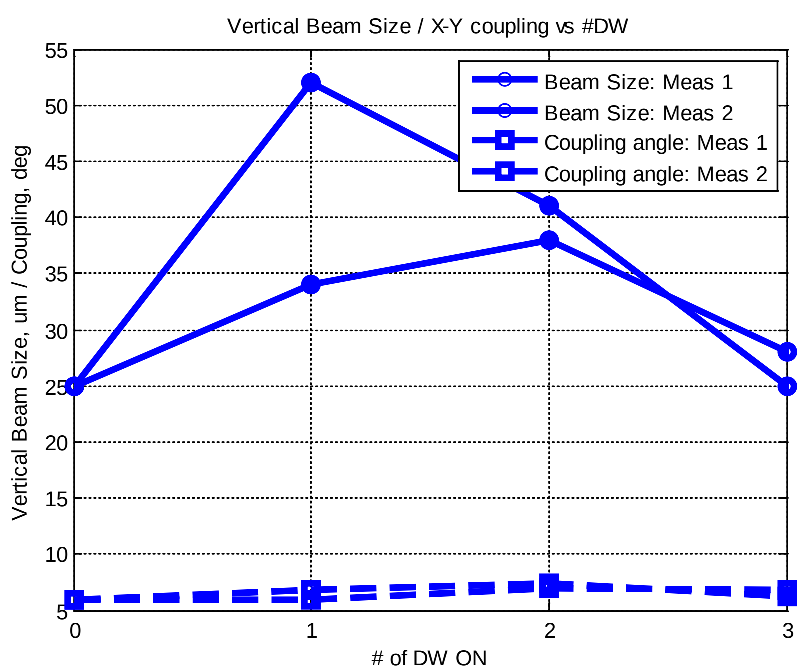

Fig. 5: Measured vertical beam size in microns for sequences #1 and #2 (circles) and X-Y

angular correlation (squares) in degrees

Throughout the measurement the tilt angle of the beam footprint observed by the X-ray diagnostics did not change significantly (Fig. 5). Thus the changes in the vertical beam size appear to happen not due to transverse coupling induced by DWs. As we discussed in the previous section of this paper, the beta-beat is small so that it may not be held responsible for the observed effect either. Our conjecture is that the vertical dispersion generated by the IDs is increasing the beam size. Indeed, 1 cm of the vertical dispersion induces about of 10 um of the beam size. We also note that the dispersion wave is compensated when all three DW gaps are closed.

These changes in the vertical beam size introduce complexity in understanding of the beam lifetime dominated by the Touschek effect. The Touschek lifetime depends, in particular, on the vertical beam size, which contains contributions from both X-Y coupling and vertical dispersion. In the following discussion we used a simple model of zero vertical dispersion and the coupling coefficient equal to 1%, which is in the ball park of the coupling measured for the "bare" latttice. The beam size calculated for this level of coupling is confirmed locally by the value seen by X-ray diagnostics (25 um, both measured and calculated, compare with Fig. 5).

In the following lifetime analysis we scale the vertical beam size according to the coupling ratio without taking the spurious dispersion into account. The latter will require a separate study to measure the dispersion wave by changing the RF cavity frequency [8].

Measurements of Lifetime

While the horizontal emittance is well understood we need to gain some understanding of how the DWs impact the energy acceptance and thus the beam lifetime. The beam lifetime for the "bare" lattice was studied and found matched with the estimates [9].

In the following we measured the lifetime using BPM sum signal [10]. We closed all DWs and used several settings of the voltage on the RF cavity. The recorded results are indicated on Figure 6.

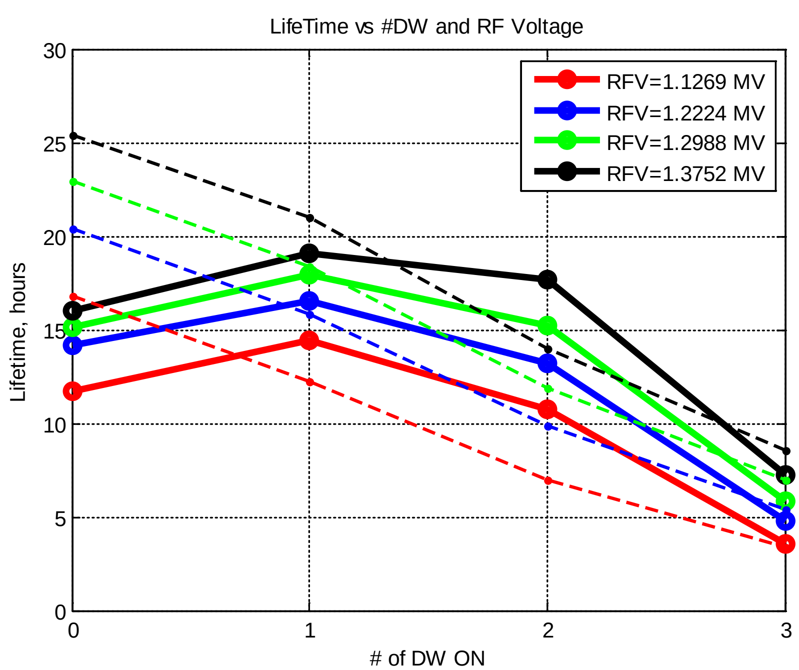

Fig. 6: Measured beam lifetime (solid traces) and Touschek fits (dashed curves) for four different RF cavity voltage values.

With the DW gaps closed the lifetime behaves in accordance with the Touschek dependence [2] since the energy acceptance becomes small (~1% at around 1.12 MV) and, thus the beam particle scattering effect dominates over other contributions. We note that the measured data scales well with respect to increasing the energy dependence as follows from Fig. 5.

For the bare lattice the agreement is far from the ideal (~50%). We believe that two mechanisms may be responsible for this worse agreement. One of them is in the uncertainty with the average vertical beam size (compare the overall shape of the lifetime trace with the measured vertical beam size presented in Fig. 5). Another one comes from contributions of the vacuum lifetime to the overall value. Having acknowledged the model-measurement deviation observed for the ring with fewer DWs we find that the measured data is quite close to the simple estimates.

References

[1] An ultra-low emittance mode for PEP using damping wigglers, H. Wiedemann, NIM A Volume 266, Issues 1–3, 1 April 1988, Pages 24–31

[2] Bruck, H., Circular Particle Accelerators, Los Alamos National Laboratory, LA-TR-72-10, Rev.

[3] Bengtsson, C. Montag and B. Nash, "Touschek Lifetime Calculations and Simulations for NSLS II," Proc. PAC '07

[4] http://www.bnl.gov/isd/documents/70446.pdf

[5] Simple determination of Touschek and beam-gas scattering lifetimes from a measured beam lifetime, Tae-Yeon Lee, Jinhyuk Choi, H.S. Kang, NIM A Volume 554, Issues 1–3, 1 December 2005, Pages 85–91

[6] W. Guo, Private Communication

[7] BNL-94868-2011, NSLS-II X-RAY DIAGNOSTICS DEVELOPMENT, http://www.bnl.gov/isd/documents/75170.pdf

[8] B. Podobedov, Private Communication and http://accelconf.web.cern.ch/AccelConf/e06/PAPERS/WEPCH016.PDF

[9] B. Podobedov in NSLS-II Commissioning Report

[10] G. Wang, Private Communication

Appendix A: Shift Data

					start current	1.5 mA	20 buckets		**RF V, MV**	**RF V, MV**	**RF V, MV**	**RF V, MV**	
									0.59	0.64	0.68	0.72	
							image		1.1269	1.2224	1.2988	1.3752	
	X-size, um	**Y-size, um**	**who**	**um error**	**eX, nm rad**	**eY (estimate)**	**coupling angle, deg**	**eX design**	**lifetime hrs**	**lifetime, hrs**	**lifetime, hrs**	**lifetime, hrs**	**error in emit X**
3DW close	60.00	28.00	Xray diag	3	0.973	0.031	6.3	0.886	3.26				0.097297297
	95.00	49.00	SLM	11									
18 and 28	65.00	38.00	Xray diag	1	1.142	0.058	7.4	1.085	7.67				0.035135135
	90.00	63.00	SLM	15									
28 closed	73.00	34.00	Xray diag	2	1.440	0.046	6.8	1.412	12.53				0.078918919
	95.00	60.00	SLM	7									
all opene	87.00	25.00	Xray diag	2	2.046	0.025	6	2.05	11.73	14.15	15.16	15.99	0.094054054
	100.00	45.00	SLM	15									
18 closed	73.00	41.00	Xray diag	2	1.440	0.841	6	1.412	14.41	16.57	17.97	19.12	0.078918919
	94.00	53.00	SLM	20									
8 and 18 c	63.00	52.00	Xray diag	2	1.073	1.352	7	1.085	10.74	13.2	15.2	17.7	0.068108108
	110.00	58.00	SLM	18									
3 DW clos	61.00	25.00	Xray diag	2	1.006	0.313	6.8	0.886	3.52	4.79	5.84	7.28	0.065945946
	90.00	66.00	SLM	22									
					final current	1.36 mA	20 buckets						

Note: do not trust estimate on vert emittance -- data not processed yet

Appendix B: Analytic Estimates

Emittance, energy spread and lifetime with damping wigglers at NSLS-II

T. Shaftan
12/4/2014

wiggler length, m	bend rad w, m	period w, m	ave beta x, m	ave beta y, m
$L_w := 0, 7 .. 56$	$\rho_w := \frac{10}{1.85}$	$\lambda_w := 0.1$	$\beta_x := 20.46$	$\beta_z := 3.36$

synch. integrals bare

$I_{1b} := 0.287282$ m

$I_{2b} := 0.251135$ 1/m

$I_{3b} := 0.01003771$ 1/m2

$I_{4b} := -0.0002297538$ 1/m

$I_{5b} := 0.00003970983$ 1/m

$\varepsilon_{xb} := 2.05$

emittance, bare nm rad

$\sigma_{Eb} := 0.51 \cdot 10^{-1}$

energy spread, bare %

synch. integrals, wiggler

$I_{2w}(L_w) := L_w \cdot \left(2 \cdot \rho_w^2\right)^{-1}$

$I_{3w}(L_w) := 4 \cdot L_w \cdot \left(3 \cdot \pi \cdot \rho_w^3\right)^{-1}$

$I_{4w} := 0$

$I_{5w}(L_w) := \lambda_w^2 \cdot \beta_x \cdot L_w \cdot \left(15 \cdot \pi^3 \cdot \rho_w^5\right)^{-1}$

$$\varepsilon_x(L_w) := \varepsilon_{xb} \cdot \left(1 + \frac{I_{5w}(L_w)}{I_{5b}}\right) \cdot \left(1 + \frac{I_{2w}(L_w) - I_{4w}}{I_{2b} - I_{4b}}\right)^{-1}$$

$$\sigma_{Ex}(L_w) := \sigma_{Eb} \cdot \left[\left(1 + \frac{I_{3w}(L_w)}{I_{3b}}\right) \cdot \left(1 + \frac{2 \cdot I_{2w}(L_w) + I_{4w}}{2 \cdot I_{2b} + I_{4b}}\right)^{-1}\right]^{0.5}$$

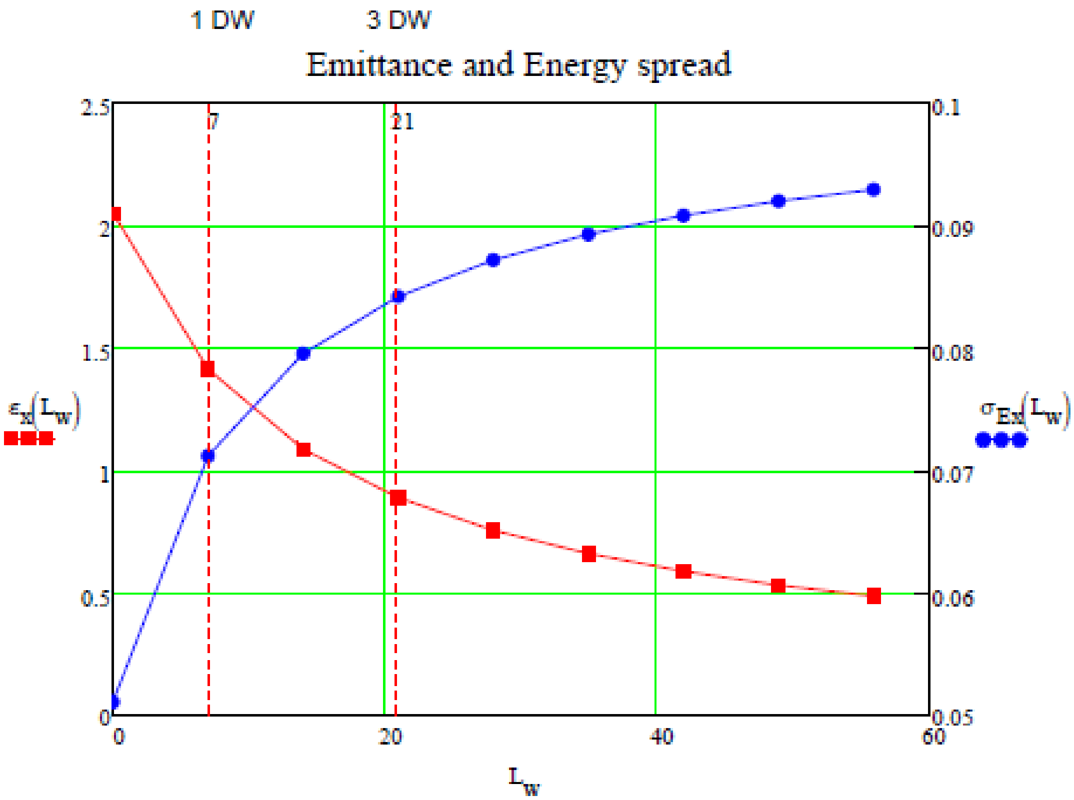

Longitudinal and RF aspects

Assume only 1 cavity

$Urfn := 1.12\cdot10^{6}$ RF Voltage, V $C_\gamma := 8.846\cdot10^{-5}$

$C_r := 792$ Cirecumference, m

$f\_RF := 500\times10^{6}$ RF frequency, Hz

$cc := 3\cdot10^{8}$ Speed of light, m/s

$T_0 := C_r\cdot cc^{-1} = 2.64\times10^{-6}$ Revolution time, s

$E\_ex := 3\cdot10^{9}$ $\gamma := \frac{E\_ex}{0.511\cdot10^{6}} = 5.871\times10^{3}$ Energy, eV

$h := \frac{C_r}{cc}\cdot f\_RF = 1.32\times10^{3}$ Harmonic number

$\alpha := 3.63\cdot10^{-4}$ Momentum compaction

$Bw := 1.85$ Field in wiggler, T

$BR := \frac{E\_ex}{3\cdot10^{8}} = 10$ Magnetic rigidity, T m

$I2w := Lw\cdot\left(2\cdot\rho_w{}^2\right)^{-1} = 0.359$ $\frac{Bw^2\cdot Lw}{2\cdot BR^2} = 0.359$ 2nd Synchr integral with DWs, 1/m

$E\_SR := 88.9\cdot10^{3}\cdot\left(\frac{E\_ex}{10^{9}}\right)^{4}\cdot\frac{I_{2b}}{(2\cdot\pi)} = 2.878\times10^{5}$ $E\_DW := 88.9\cdot10^{3}\cdot\left(\frac{E\_ex}{10^{9}}\right)^{4}\cdot\frac{I2w}{2\cdot\pi} = 4.119\times10^{5}$

$E\_T := E\_SR + E\_DW = 6.997\times10^{5}$ Total radiated energy, eV

$\phi sn := asin\left[\left(\frac{Urfn}{E\_T}\right)^{-1}\right] = 0.675$ synchronous phase $\phi sn\cdot\frac{180}{\pi} = 38.66$

$fsn := \frac{cc}{C_r}\cdot\sqrt{\frac{\alpha\cdot h\cdot\cos(\phi sn)\cdot Urfn\cdot10^{3}}{2\cdot\pi\cdot E\_ex\cdot1000}} = 1.786\times10^{3}$ synchrotron frequency, Hz

$\sigma tn := \frac{\alpha\cdot 1}{2\cdot\pi\cdot fsn}\cdot\sigma_{Ex}(Lw)\cdot10^{-2} = 2.722\times10^{-11}$ bunch length in s

RF acceptance:

$qn := \frac{Urfn}{E\_T} = 1.601$ Overvoltage

$\varepsilon RFn := \left[\frac{2 \cdot E\_T}{\pi \cdot \alpha \cdot h \cdot E\_ex} \cdot \left(\sqrt{qn^2 - 1} - acos\left(\frac{1}{qn}\right)\right)\right]^{0.5} = 0.01047$ energy acceptance

Quantum lifetime

$a_s := \frac{E\_T}{2 \cdot E\_ex \cdot T_0} \cdot 2 = 88.342$ damping factor, 1/s

$\tau_E := \frac{1}{a_s} = 0.011$ damping time, s

$r_s := \frac{1}{2} \cdot \left(\frac{\varepsilon RFn}{\sigma_{Ex}(Lw) \cdot 10^{-2}}\right)^2$

$\tau_q := \frac{1}{2 \cdot a_s \cdot r_s} \cdot \exp(r_s) \cdot \frac{1}{3600} = 8.482 \times 10^{25}$ hrs

General constants and parameters

$r0 := 2.817940325 \cdot 10^{-15}$ Classical electron radius, m

$e := 1.60217653 \cdot 10^{-19}$ Electron charge, C

$N_b := 20$ Number of bunches

$I0 := \frac{1.5}{N_b} \cdot 10^{-3}$ Single bunch current, A

$N0 := \frac{I0 \cdot C_r}{e \cdot cc} = 1.236 \times 10^9$ Number of electrons per bunch

$\sigma zn := \sigma tn \cdot c = 8.162 \times 10^{-3} \frac{m}{s}$ Bunch length, m

$Lw := 21$ Total length of wigglers, m

$$\varepsilon_{xb} \cdot \left(1 + \frac{I_{5w}(Lw)}{I_{5b}}\right) \cdot \left(1 + \frac{I_{2w}(Lw) - I_{4w}}{I_{2b} - I_{4b}}\right)^{-1} = 0.886$$

emittance and energy spread at this compliment of DWs

$$\sigma_{Eb} \cdot \left[\left(1 + \frac{I_{3w}(Lw)}{I_{3b}}\right) \cdot \left(1 + \frac{2 \cdot I_{2w}(Lw) + I_{4w}}{2 \cdot I_{2b} + I_{4b}}\right)^{-1}\right]^{0.5} = 0.084$$

Coupling $\kappa := 0.01$

Vertical emittance nm rad

$$\varepsilon_y := \frac{\kappa \cdot \varepsilon_x(Lw)}{1 + \kappa} = 8.775 \times 10^{-3}$$

Calculated transverse beam size

$LD1 :=$ lattice.txt

$NJ_{lp} := 179$ $j := 0 .. NJ_{lp}$ $\beta xJ_j := LD1_{j,4}$ $\beta yJ_j := LD1_{j,11}$

$sJ_j := LD1_{j,3}$ $\eta xJ_j := LD1_{j,9}$ $\eta xpJ_j := LD1_{j,10}$

$\alpha xJ_j := LD1_{j,5}$

$$sxJ_j := \sqrt{\beta xJ_j \cdot \varepsilon_x(Lw) \cdot 10^{-9} + \left(\eta xJ_j \cdot \sigma_{Ex}(Lw) \cdot 10^{-2}\right)} \quad syJ_j := \sqrt{\beta yJ_j \cdot \varepsilon_y \cdot 10^{-9}}$$

$$sa := \sum_j sJ_j \qquad xa := \frac{1}{sa} \cdot \sum_j \left(sxJ_j \cdot sJ_j\right) = 1.717 \times 10^{-4} \qquad ya := \frac{1}{sa} \cdot \sum_j \left(syJ_j \cdot sJ_j\right) = 1.104 \times 10^{-5}$$

$ss := 0 .. sJ_{NJ_{lp}}$ $sJ_{NJ_{lp}} = 52.797$

$SX := \text{pspline}(sJ, sxJ)$ $fitX(ss) := \text{interp}(SX, sJ, sxJ, ss)$

$SY := \text{pspline}(sJ, syJ)$ $fitY(ss) := \text{interp}(SY, sJ, syJ, ss)$

$$xa := \frac{1}{sJ_{NJ_{lp}}} \cdot \int_0^{sJ_{NJ_{lp}}} fitX(x)\, dx = 1.381 \times 10^{-4}$$

Vertical marker indicates the X-ray diagnostics location

$fitX(19.3) = 5.7 \times 10^{-5}$ $fitY(19.3) = 1.481 \times 10^{-5}$

$$ya := \frac{1}{sJ_{NJ_{lp}}} \cdot \int_0^{sJ_{NJ_{lp}}} fitY(x)\, dx = 1.04 \times 10^{-5}$$

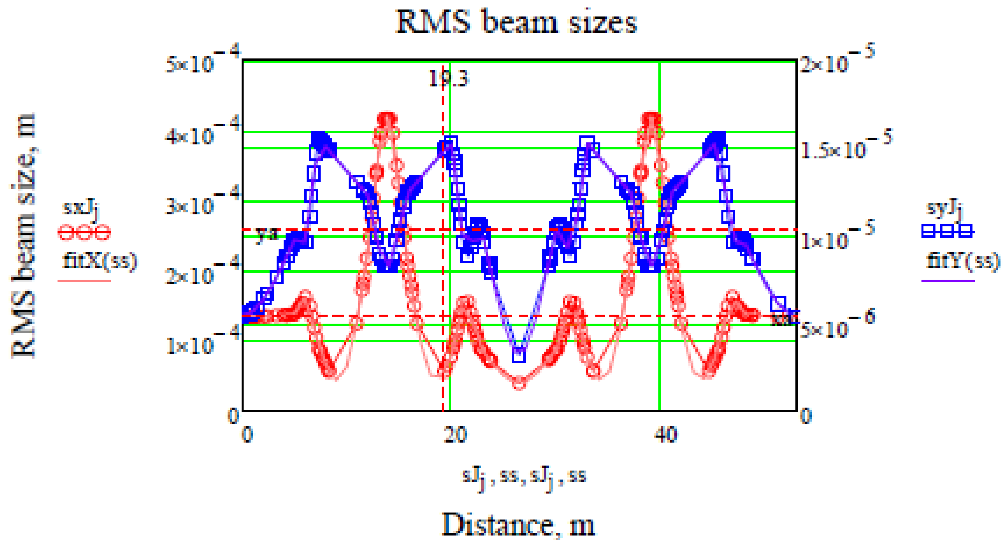

average x beta-function, m $\beta xav := \frac{1}{sa} \cdot \sum_{j} \left(\beta xJ_j \cdot sJ_j \right) = 14.286$

$BX := cspline(sJ, \beta xJ)$ $fitBX(ss) := interp(BX, sJ, \beta xJ, ss)$

$BY := cspline(sJ, \beta yJ)$ $fitBY(ss) := interp(BY, sJ, \beta yJ, ss)$

$\beta xav := \frac{1}{sJ_{NJ_{lp}}} \cdot \int_0^{sJ_{NJ_{lp}}} fitBX(x)\, dx = 12.203$ $\beta yav := \frac{1}{sJ_{NJ_{lp}}} \cdot \int_0^{sJ_{NJ_{lp}}} fitBY(x)\, dx = 13.568$

$$H_j := \frac{\left[1 + \left(\alpha xJ_j\right)^2\right]}{\beta xJ_j} \cdot \left(\eta xJ_j\right)^2 + 2 \cdot \alpha xJ_j \cdot \eta xJ_j \cdot \eta xpJ_j + \beta xJ_j \cdot \left(\eta xpJ_j\right)^2$$

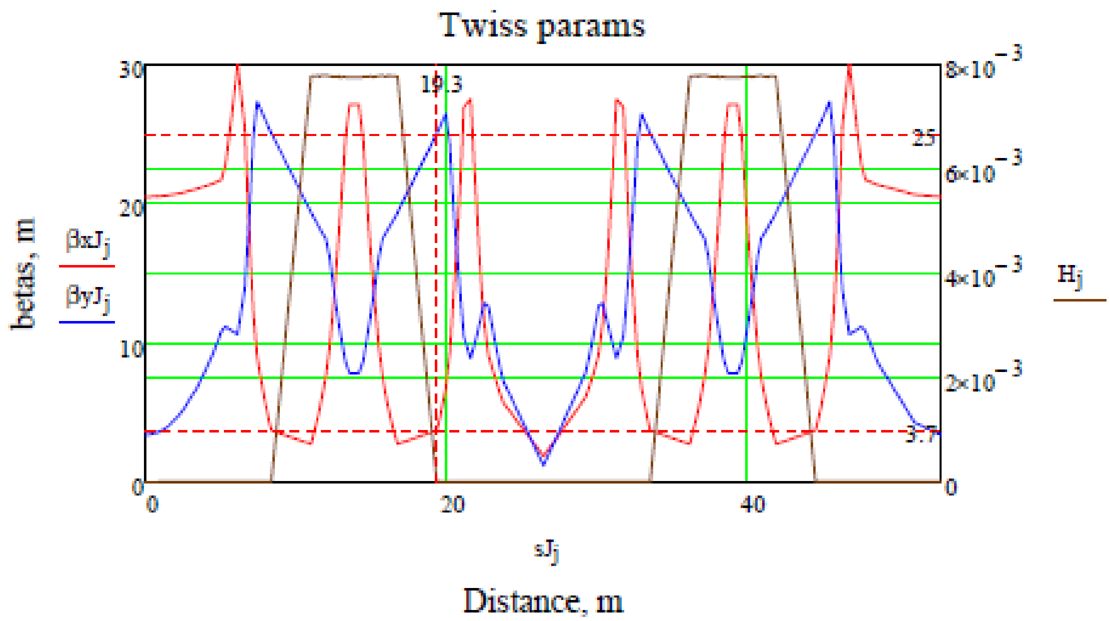

$\sigma xpd_j := \frac{\epsilon_x(Lw) \cdot 10^{-9}}{sxJ_j} \cdot \sqrt{1 + \frac{H_j \cdot \sigma_{Ex}(Lw)^2}{\epsilon_x(Lw)} \cdot 10^5}$

Average beam divergence, rad

$\sigma xpc := \sqrt{\epsilon_x(Lw) \cdot 10^{-9} \cdot \beta xav^{-1}} = 8.522 \times 10^{-6}$

$Bxp := cspline(sJ, \sigma xpd)$

$fitBxp(ss) := interp(Bxp, sJ, \sigma xpd, ss)$

$\sigma xp := \frac{1}{sJ_{NJ_{lp}}} \cdot \int_0^{sJ_{NJ_{lp}}} fitBxp(x)\, dx = 1.199 \times 10^{-5}$

Touschek Lifetime

$$f(\varepsilon) := 0.5\cdot\int_0^1 \left(\frac{2}{u} - \ln\left(\frac{1}{u}\right) - 2\right)\cdot\exp\left(-\frac{\varepsilon}{u}\right)du$$ Bruck

$$\tau TS(x) := \frac{8\cdot\pi\cdot\gamma^3\cdot\sigma zn\cdot xa\cdot\sigma xp\cdot ya\cdot x^2}{N0\cdot r0^2\cdot c\cdot f\left[\left(\frac{x}{\gamma\cdot\sigma xp}\right)^2\right]}\cdot\frac{1}{3600}$$ $\tau TS(\varepsilon RFn) = 3.771$ hours

$2.817940325^2\cdot 299792458\cdot N0 = 2.942\times 10^{18}$ Coefficient in Bruck's formula

Auxilliary estimates

$Vo := 8\cdot\pi^{\frac{3}{2}}\cdot xa\cdot ya\cdot\sigma zn\cdot 3 = 1.567\times 10^{-9}\,\frac{m}{s}$ Electron beam volume, m^3

This is the integral by Bruck again from R.P. Walker, PAC-1987, pp. 491 - 493

$$CW(\varepsilon) := -\frac{3}{2}\cdot\exp(-\varepsilon) + \frac{\varepsilon}{2}\cdot\int_{\varepsilon}^{\infty}\frac{\ln(u)}{u\cdot\exp(u)}du + \frac{(3\cdot\varepsilon - \varepsilon\cdot\ln(\varepsilon) + 2)}{2}\cdot\int_{\varepsilon}^{\infty}\frac{1}{u\cdot\exp(u)}du$$

$$\tau TB(x) := \frac{\sigma xp\cdot\gamma^3\cdot x^2\cdot 8\cdot\pi^{1.5}\cdot\sigma zn\cdot xa\cdot ya}{\sqrt{\pi}\cdot N0\cdot r0^2\cdot c\cdot CW\left[\left(\frac{x}{\gamma\cdot\sigma xp}\right)^2\right]}\cdot\frac{1}{3600}$$ $\tau TB(\varepsilon RFn) = 3.771$ hours

Parameter of interest:

$$\left(\frac{\varepsilon RFn}{\gamma\cdot\sigma xp}\right)^2 = 0.022$$

Comparison between two integrals by Bruck

$yy := 0.01, 0.02 .. 0.5$